Available online at www.sciencedirect.com
SCIENCE DIRECT
Journal of Organometallic Chemistry 691 (2006) 2793–2809
Journal of Organometallic Chemistry
www.elsevier.com/locate/jorganchem

Anion binding with some 22- and 28-membered selenaaza macrocycles: Structural aspects and ^{77}Se NMR studies

Snigdha Panda [a], Sanjio S. Zade [a], Arunashree Panda [a], Harkesh B. Singh [a,*], Ray J. Butcher [b]

[a] *Department of Chemistry, Indian Institute of Technology Bombay, Powai, Mumbai 400 076, India*
[b] *Department of Chemistry, Howard University, Washington, DC 20059, USA*

Received 4 April 2005; received in revised form 11 November 2005; accepted 15 February 2006
Available online 6 March 2006

Abstract

A series of macrocyclic adducts of the 22- and 28-membered selenaaza macrocycles (**1** and **2**, respectively) with different counter anions such as halides, sulfate, perchlorate, phosphate, trifluoroacetate and nitrate has been prepared. The adducts have been characterized by elemental analysis, IR, ^{1}H NMR, ^{77}Se NMR and ESI-MS analysis. The ^{77}Se NMR spectrum of the SO_4^{2-} adduct (**7**) shows an upfield shift compared to the parent macrocycle. The bromo (**5**), iodo (**6**), sulfate (**7**), trifluroacetate (**10**) adducts of the 22-membered selenaaza macrocycle and perchlorate (**16**), trifluroacetate (**18**) adducts of the 28-membered selenaaza macrocycle have been structurally characterized. The crystal structures show extensive hydrogen bonding networks. The molecular structures of all the compounds show the macrocycle to be fully protonated except the trifluroacetate adduct of the 22-membered macrocycle (**10**), which is only diprotonated. The binding constants of the neutral 22-membered selenaaza macrocycle towards, fluoride, bromide, iodide and sulfate ion have been determined by the NMR titration method.

Keywords: Selenaaza macrocycles; ^{77}Se NMR; Anion binding; EQNMR; Hydrogen bonding

1. Introduction

The molecular recognition of the anions with synthetic receptors is an expanding field of research [1]. Synthetic anion receptors, to date, have typically employed various combinations of Lewis acids [2], pyrroles [3], guanidiniums [4], amides [5] and polyammonium macrocycles [6]. The selectivity of these hosts comes from both the size and shape complementarity as well as the anion basicity. The polyamine macrocycles can act as receptors for cations, neutral molecules as well as anions. These polyamine macrocycles are capable of undergoing polyprotonation in solution forming positively charged polyammonium cations, which can bind selectively a variety of inorganic, organic and biologically important anions by electrostatic forces and hydrogen bonding.

The chalcogen (Se, Te) atoms exhibit weak intra- or inter-molecular chalcogen–X (X = nitrogen [7], chalcogen [8], phosphorous [9], hydrogen [10], fluorine [11], iodine [12]) interactions. The heavier chalcogens (Se,Te) are more prone towards secondary interactions than sulfur. In particular, the chemistry of tellurium has numerous examples of ''intramolecular coordination'' in its derivatives such as diazenes, Schiff bases, pyridines, amines, and carbonylic compounds [10d]. We thought that the incorporation of selenium into the azamacrocycles should show selectivity in anion binding compared to the simple azamonocycles due to; (i) the geometrical arrangement required around Se is V-shape, which would lead to a puckered structure instead of a flat one for the monocycle. The puckered structure is more effective towards anion binding. (ii) The strong propensity of selenium for secondary interactions with

* Corresponding author. Tel.: +91 22 2576 7190; fax: +91 22 2572 3480.
E-mail address: chhbsia@chem.iitb.ac.in (H.B. Singh).

0022-328X/$ - see front matter © 2006 Elsevier B.V. All rights reserved.
doi:10.1016/j.jorganchem.2006.02.016

heteroatoms should lead to a better binding/recognition of anions. (iii) The Se(II) can be easily ternarnised to give additional cationic centers of interaction with the anions. (iv) Se in a macrocycle will provide an additional tool for studying the binding capability of macrocycle towards anions. The selenium anion interactions can be easily monitored by the shift in the ^{77}Se NMR resonances; the magnitude of this shift corresponds approximately to the strength of the interaction. There are very few reports about chalcogen containing hosts for molecular recognition. Recently Liu et al. [13] have studied the molecular recognition properties of organoselenium-bridged bis(β-cyclodextrins) and emphasized that the selenium bridge acts as a versatile coordinating site that can control the orientation and binding selectivity of the bis(cyclodextrins). Giolando et al. have reported a novel cage organotellurate(IV) macrocylic host encapsulating a bromide ion [14]. We have developed selenium containing aza-macrocycles **1**, **2** and studied their complexation properties towards various metal ions [15,16]. In this paper we report the anion adduct formation properties of the protonated and neutral selenaaza macrocycles of different ring sizes with various anions such as halides, SO_4^{2-}, ClO_4^-, PO_4^{3-}, CF_3COO^- and NO_3^-.

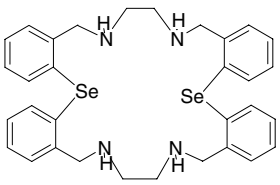

1

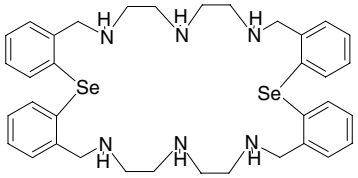

2

2. Results and discussion

2.1. Syntheses

The ligands **1** and **2** were prepared by following the known procedure [15]. Compounds **3**–**19** were synthesized as white solids by treating the ligands **1** and **2** with the corresponding acids. All the compounds are insoluble in common chlorinated solvents and poorly soluble in protic solvents, however, some compounds (**3**–**8**, **10**, **12**–**14**, **16**, **18**) are soluble in protic solvents (DMSO/MeOH/EtOH/H_2O) on heating. The elemental analysis data show the presence of water molecules in case of most of the adducts, which has been further confirmed by single crystal X-ray crystallographic studies (vide infra). These compounds are well characterized by IR, ESI-MS and solution multinuclear NMR spectroscopic techniques. The reaction of methyl iodide with **1** was attempted to prepare the chalcogenonium form of the macrocycle, which in turn should be a better anion receptor due to the presence of positive charge on the selenium atoms in addition to nitrogens. However, all attempts to react **1** with an excess of MeI (>6 fold) were unsuccessful in obtaining the chalcogenonium form, instead the reaction afforded the tetraprotonated compound **6**. The formation of the product **6** may be explained in terms of formation of HI during the alkylation reaction of the secondary amines, which reacts more aggressively than methyl iodide [17]. Also the attempted methylation of the macrocycle in presence of the base lutidine afforded a mixture of product, which were found to be inseparable.

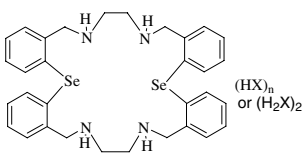

$(HX)_n$ or $(H_2X)_2$

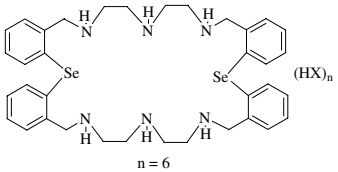

$(HX)_n$

n = 6

3 X = F^-, n=4
4 X = Cl^-, n=4
5 X = Br^-, n=4
6 X = I^-, n=4
7 X = SO_4^{-2}, n=2
8 X = ClO_4^-, n=4
9 X = $H_2PO_4^-$, n=4
10 X = CF_3COO^-, n=2
11 X = NO_3^-, n=4

12 X = F^-
13 X = Cl^-
14 X = I^-
15 X = HSO_4^-
16 X = ClO_4^-
17 X = $H_2PO_4^-$
18 X = CF_3COO^-
19 X = NO_3^-

2.2. Spectroscopic studies

FT-IR spectra of all the compounds give information about the N–H stretching frequencies of the macrocycles, and the presence of the oxo-anions SO_4^{2-} or HSO_4^-, ClO_4^-, $H_2PO_4^-$, CF_3COO^- and NO_3^-. The IR spectra of the parent tetraamines **1** and **2** show sharp peaks in the region 3320–3236 cm^{-1} corresponding to the ν(N–H) stretching vibrations. Whereas on adduct formation with anions, the N–H stretching vibrations appeared at 2700–3100 cm^{-1} as broad multiplets corresponding to the characteristic vibrations for the secondary ammonium cations. For adducts **7** and **15** the peaks at 1459 and 1438 cm^{-1}, respectively, correspond to S=O stretching vibration. For adducts **8** and **16** the observation of peaks at 1090 and 626 cm^{-1}, 1088 and 626 cm^{-1}, respectively, corresponds to the presence of ClO_4^- ion. In adducts **9** and **17** the peaks at 945 and 975 cm^{-1} correspond to P–O stretching frequency and the peaks at 2370 and 2388 cm^{-1} correspond to O=P–OH stretching frequency. The IR spectra of **10** and **18** showed the peaks consistent with the presence of coordinated carboxylate group with ν_{COO} at 1650 and 1675 cm^{-1}, respectively. For adducts **11** and **19** the infrared spectra show the corresponding peak at 1380 cm^{-1} for the presence of N–O stretching frequency in NO_3^-.

ESI-mass spectra of the anion adducts were recorded to identify the constitution of the anion adducts under mass spectroscopic conditions. For all compounds the peaks

for the molecular ion are observed in low intensity, however the highest intensity peaks are observed for the cationic macrocycles.

The ^{1}H NMR spectra of the compounds were recorded in DMSO-d_6,CD_3OD, or D_2O. For compounds **3**–**10** and **11** the Ar–CH_2 signals spanned a range of δ 3.9–4.75 and NH–CH_2 signals spanned a range of δ 2.82–3.68 showing considerable downfield shifts compared with the free macrocycle **1** (δ 3.85 for Ar–CH_2 and 2.71 for NH–CH_2). For compounds **12**–**19** the Ar–CH_2 signals spanned a range of δ 4.46–4.61 and NH–CH_2 signals spanned a range of δ 3.38–3.70 as multiplets showing considerable downfield shifts compared with the free macrocycle **2** (δ 3.87 (s) for Ar–CH_2 and 2.7 (m) for NH–CH_2). On comparing the shifts in ^{1}H NMR spectra of adducts of ligand **1** and **2**, no significant difference was observed between adducts of the two macrocycles.

The ^{77}Se NMR spectra of the compounds were recorded in DMSO-d_6, D_2O, or CD_3OD solutions. The observation of single signals for each of adducts confirms the equivalence of two selenium atoms. There is no significant difference in ^{77}Se NMR chemical shifts of halide adducts **3**–**6** compared to the parent macrocycle **1**. The small changes observed (~2–5 ppm) may be due to the solvent effect. Interestingly, the sulfate derivative **7** shows a considerable upfield shift in the ^{77}Se NMR ($\delta = 88$ ppm) compared to the parent ligand ($\delta = 329$ ppm), which may be due to dianionic nature of the sulfate ion. It is not surprising that the analogous hydrogen sulfate adduct **15** (with single negative charge) of the larger ring macrocycle does not show a comparable shift in the ^{77}Se NMR spectrum. Other oxoanion adducts (**8**, **11**, **15**–**17**, **19**) show a small upfield shift of ~19 ppm compared to the parent ligands indicating that there may be a very weak interaction between the anion and the Se atoms in the solution state. The trifluroacetate derivatives **10** and **18** did not show any significant shift compared to the parent ligands.

2.3. X-ray crystallographic studies

A summary of the data collection and refinement parameters for compounds **5**, **6** and **7** are listed in Table 1 and that of **10**, **16** and **18** are listed in Table 2. The crystal structure of **15** could not be satisfactorily solved due to high disorder of the hydrogen sulfate ion.

2.3.1. Molecular structure of compound 5

The ORTEP diagram with atomic labeling is shown in Fig. 1. Table 3 gives the hydrogen bond distances in the molecule. Compound **5** crystallizes with three water molecules of crystallization. The unit cell consists of two discrete molecules with extensive hydrogen bonding among the neighbouring molecules. The macrocycle framework is tetraprotonated. The molecular structure is centrosymmetric and only half of the molecules represent the asymmetric unit. The macrocyclic framework is highly puckered ellipsoid so as to suit the bonding pattern of the individual atoms. Out of the four-phenyl rings, one *trans* pair is canted down the plane of the ring whereas the other pair is canted above the plane of the ring. The transannular Se...Se distance is 7.286 Å, which is far greater than the sum of the van der Waals radii of the selenium atoms.

In **5** none of the bromide counter ions are situated inside the macrocyclic cavity, but one lies above the macrocyclic plane and forms intermolecular hydrogen bonding with NH_2^+ and the hydrogens of a water molecule (Table 3). One of the nitrogens is having bifurcated hydrogen bonding with two bromine atoms and the other nitrogen atom is bonded to one bromine and one water molecule. The N–H...Br hydrogen-bonding interactions in **5**

Table 1
Crystal data and structure refinement of **5**, **6** and **7**

	5	**6**	**7**
Empirical formula	$C_{32}H_{46}Br_4N_4O_3Se_2$	$C_{32}H_{44}I_4N_4O_2Se_2$	$C_{32}H_{40}N_4O_9S_2Se_2$
F_w	1012.29	1182.23	846.72
Crystal system	Monoclinic	Monoclinic	Monoclinic
Space group	*P2/n*	*P2/n*	*P2/n*
a (Å)	10.7586(11)	10.8628(6)	14.272(3)
b (Å)	7.3605(8)	7.6435(4)	5.3331(10)
c (Å)	24.330(3)	24.5655(13)	26.363(5)
α (°)	90	90	90
β (°)	96.406(2)	95.0200(10)	95.749(3)
γ (°)	90	90	90
V (Å^3)	1914.6(3)	2031.84(19)	1996.4(7)
Z	2	2	2
Temperature (K)	168(2)	293(2)	93(2)
Absorption coefficient (mm^{-1})	6.141	4.890	2.008
Observed reflections [$I > 2\sigma$]	4514	4968	5027
Final $R(F)$ [$I > 2\sigma$][a]	0.0325	0.0487	0.1051
$wR(F^2)$ indices [$I > 2\sigma$]	0.0603	0.1226	0.3045

[a] Definition: $R(F_o) = \sum||F_o| - |F_c||/\sum|F_o|$ and $wR(F_o^2) = \{\sum[w(F_o^2 - F_c^2)^2]/\sum[w(F_c^2)^2\}^{1/2}$.

Table 2
Crystal data and structure refinement of **10**, **16** and **18**

	10	**16**	**18**
Empirical formula	$C_{36}H_{38}F_6N_4O_4Se_2$	$C_{36}H_{70}C_{l6}N_6O_{33}Se_2$	$C_{48}H_{60}F_{18}N_6O_{16}Se_2$
F_w	862.62	1485.60	1476.94
Crystal system	Orthorhombic	Monoclinic	Triclinic
Space group	*Fdd*2	$P2_1/m$	$P\bar{1}$
a (Å)	13.6270(13)	7.6167(5)	9.389(2)
b (Å)	43.496(5)	31.034(2)	10.636(2)
c (Å)	12.3646(13)	12.9377(9)	16.500(4)
α (°)	90	90	104.059(4)
β (°)	90	99.1000(10)	101.745(4)
γ (°)	90	90	101.100(5)
V (Å^3)	7328.7(13)	3019.7(4)	1513.3(6)
Z	8	2	1
Temperature (K)	168(2)	293(2)	293(2)
Absorption coefficient (mm^{-1})	2.093	1.585	1.346
Observed reflections [$I > 2\sigma$]	3910	7731	11 067
Final $R(F)$ [$I > 2\sigma$][a]	0.0330	0.1023	0.0802
$wR(F^2)$ indices [$I > 2\sigma$]	0.0666	0.2761	0.1777

[a] Definition: $R(F_o) = \sum||F_o| - |F_c||/\sum|F_o|$ and $wR(F_o^2) = \{\sum[w(F_o^2 - F_c^2)^2]/\sum[w(F_c^2)^2\}^{1/2}$.

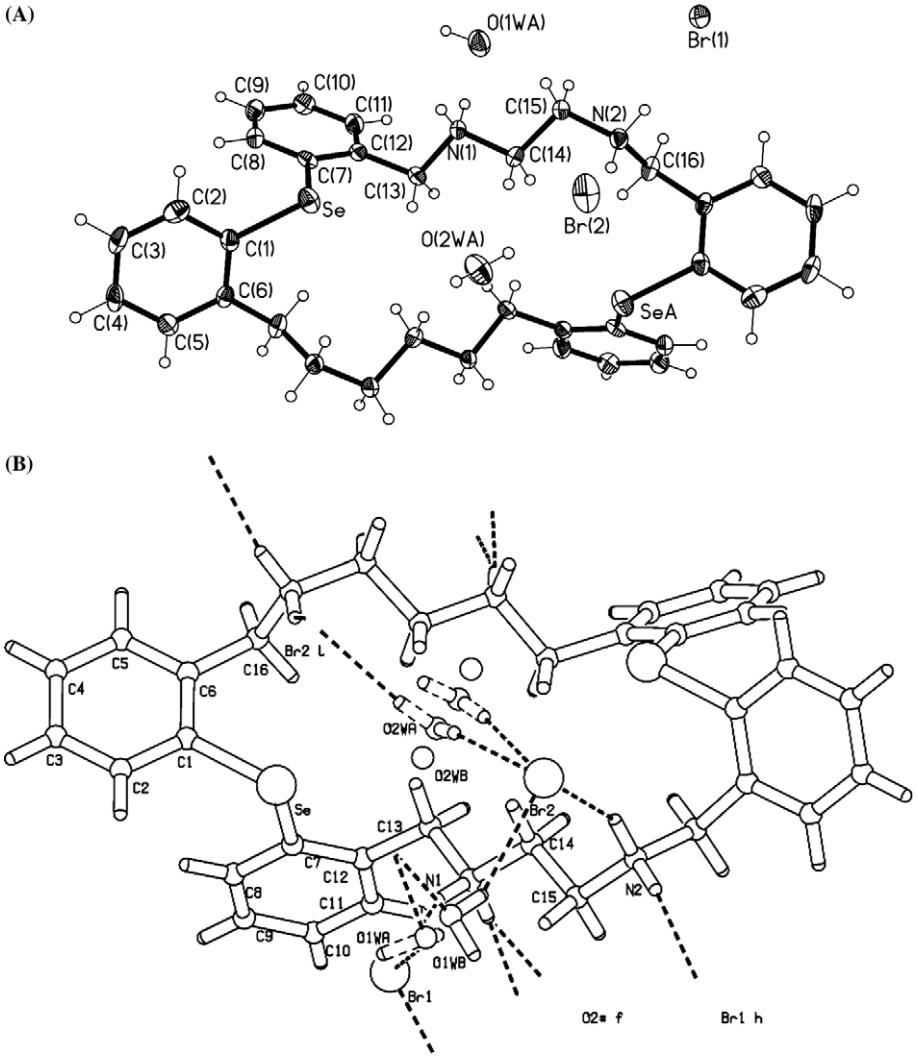

Fig. 1. (A) Side view of compound **5**. (B) Overhead view of compound **5**.

Table 3
Hydrogen bonds for **5** (Å and °)

D–H...A	*d*(D–H)	*d*(H...A)	*d*(D...A)	∠(DHA)
O(1WA)–H(1WA)...Br(1)#2	0.858(10)	2.74(3)	3.456(7)	142(4)
O(1WB)–H(1WB)...Br(2)#3	0.847(10)	2.48(3)	3.174(6)	140(4)
O(1WB)–H(2WB)...O(1WB)#4	0.845(10)	2.07(4)	2.814(14)	147(5)
O(2WA)–H(3WA)...Br(2)#1	0.850(10)	2.49(3)	3.276(12)	154(5)
O(2WA)–H(4WA)...Br(2)	0.850(10)	2.403(18)	3.248(12)	173(7)
N(1)–H(1A)...O(1WA)	0.92	1.88	2.789(7)	169.0
N(1)–H(1A)...O(1WB)	0.92	1.94	2.841(7)	166.3
N(1)–H(1B)...Br(1)#4	0.92	2.42	3.308(2)	162.2
N(2)–H(2B)...Br(2)	0.92	2.46	3.285(3)	148.7
N(2)–H(2C)...Br(1)	0.92	2.36	3.254(2)	162.9

[N(1)–H(1B)...Br(1)#4, N(2)–H(2B)...Br(2), N(2)–H(2C)...Br(1)] are 2.42, 2.46 and 2.36 Å, respectively. These distances show that the interaction of Br(1) atom with the macrocycle is strongest. The $N^+...Br^-$ distances ~3.285(3) Å are well within the sum of the van der Waals radii 3.45 Å and are comparable to those found in similar macrocycle bromide derivatives [18].

The packing diagram (Fig. 2) shows that between two neighbouring saddle type macrocyclic frameworks, an open cage is formed by one of the bromide anions and the NH group and a water molecule is trapped in this open cage.

2.3.2. Molecular structure of compound *6*

The crystal structure (Fig. 3) of the compound shows the macrocycle to be in its tetraprotonated form. The overall macrocycle framework is isostructural to that of **5**. The transannular Se...Se distance in the case of **6** is 7.405 Å. Only some major differences in the structure will be highlighted here. N(1A) forms hydrogen bonds with I(1) and I(2) at 3.435 and 3.472 Å. I(1) forms hydrogen bond with N(1A) of one macrocycle and N(1B) nitrogen atom of an adjacent molecule. N(1B) interacts with the nearby water molecule. I(2) interacts with H atom of the adjacent water molecule. The $N^+...I^-$ distances ~3.45 Å are well within the sum of the van der Waals radii of N and I (3.65 Å). All the N^+–H...I^- interactions are almost linear. These $N^+...I^-$ bond distances, as expected, are greater than the N^+–Br^- distance observed for the **5**. The O–H...I interactions are also well within the sum of van der Waals radii of the corresponding atoms.

The overall packing diagram (Fig. 4, Table 4) shows that the water molecule is away from the iodide ion of the cage, which was inside the cage in the case of **5**. This may be due to lower electronegativity and larger size of the iodide ion compared to the bromide anion in compound **5**.

2.3.3. Molecular structure of compound *7*

The molecular structure of the compound is given in Fig. 5. The compound contains, tetraprotonated **1**, two sulfate ions and a water molecule of crystallization. The macrocyclic framework is similar to **5**. The major axis runs between C(1B)–C(1B) with a distance of 9.478 Å, whereas the minor length is N(1B)–N(1A) 4.784 Å. The transannular Se...Se bond distance is 7.322 Å. Out of the two sulfate ions, one ion is disordered.

In this compound the hydrogen-bonding interactions are interesting. The disordered sulfate ion maintains strong hydrogen bonds to all the nitrogen atoms of the macrocycle and resides just above and below the macrocycle framework. The symmetry related N atoms are hydrogen bonded to the disordered sulfate ion at the same distance. The hydrogen bond distance between N(1A) and O(11) is 2.777(10) Å

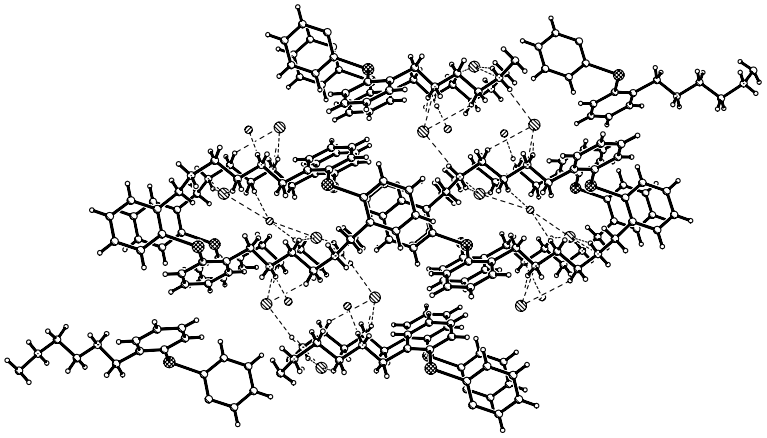

Fig. 2. Packing diagram showing hydrogen bonding for compound **5**.

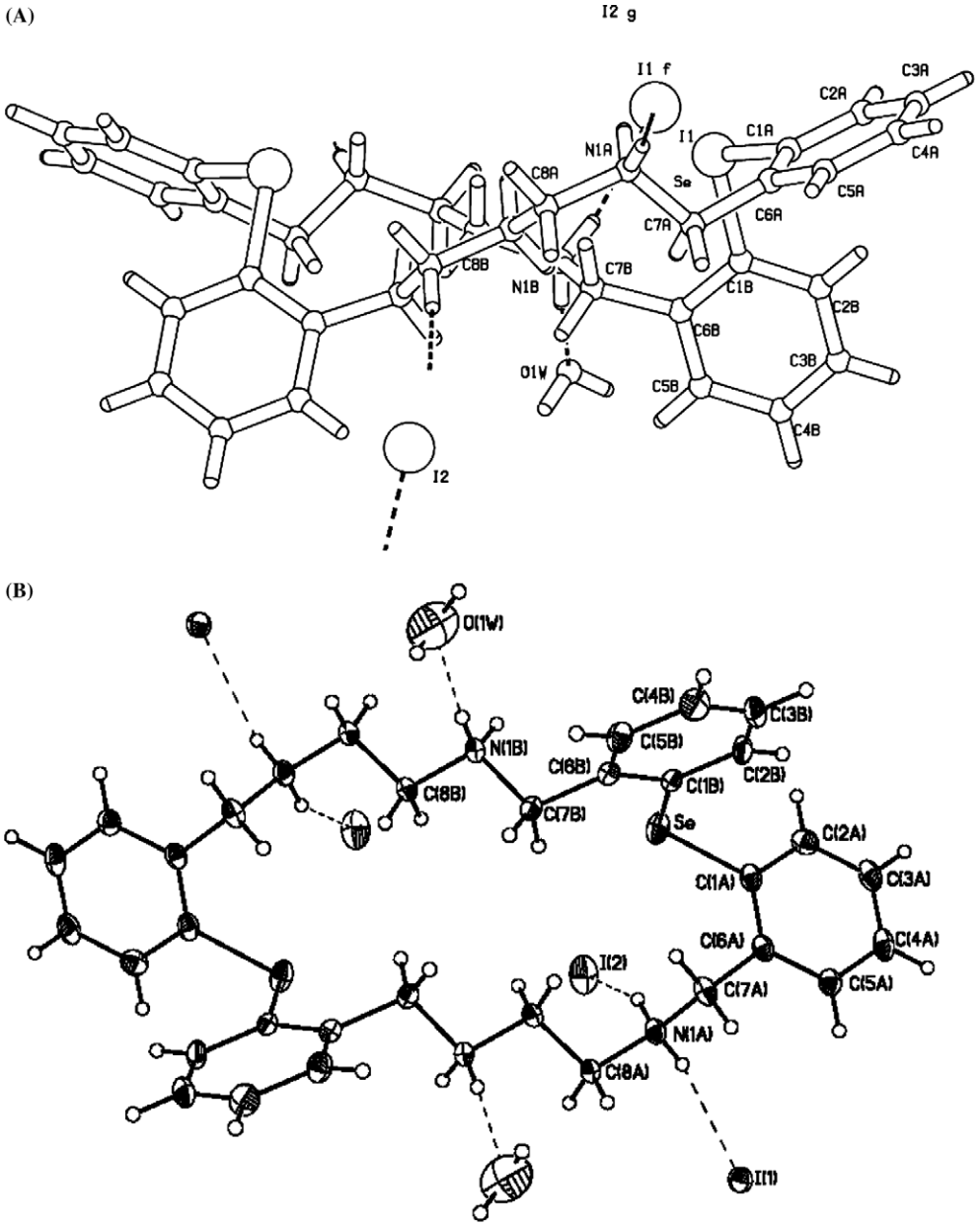

Fig. 3. (A) Side view of compound **6** showing hydrogen bonding. (B) Overhead view of compound **6** showing hydrogen bonding.

and that of N(1B) and O(12) is 2.609(12) Å. The N(1B) and O(12) hydrogen bond distance is smaller compared to the hydrogen bond distance reported for the sulfate adduct of the polyamine macrocycle (3,6,9,17,20,23-hexaazatricyclo[23.3.1.1]-triaconta-1(29).11.13,15(30), 25,27-hexaene) [19] indicating that the sulfate ion is strongly bonded to the protonated form of the macrocycle **1**. The disordered sulfate ion is also hydrogen bonded to the symmetric N(1B) nitrogen atom of the next neighboring macrocycle at a distance of 2.714(13) Å [N(1B) and O(13)] and 3.047(12) Å [N(1B) and O(12)]. The other sulfate ion is hydrogen bonded to N(2A) at a distance of 2.739(11) Å. All the hydrogen bond distances between N atoms of the macrocycle and oxygen atoms of the sulfate ion are well within the hydrogen-bonding distance of the reported sulfate ion monocycle adduct [19]. There is no direct interaction with any water molecules and the macrocycle framework. The entire packing system (Fig. 6, Table 5) forms a supramolecular arrangement by hydrogen bonding and short contacts between layers of macrocycles, sulfate anion, where the disordered sulfate ion is sandwiched between the macrocycle layers.

2.3.4. Molecular structure of compound *10*

The crystal structure (Fig. 7) of the trifluroacetate (TFA) adduct, unexpectedly, shows the macrocycle in the diprotonated form. The compound contains the diprotonated ligand **1** and two trifluroacetate counter ions. Interestingly the molecule does not contain any water molecules of crystallization. All the four phenyl rings are canted away from the plane of the macrocycle in one direc-

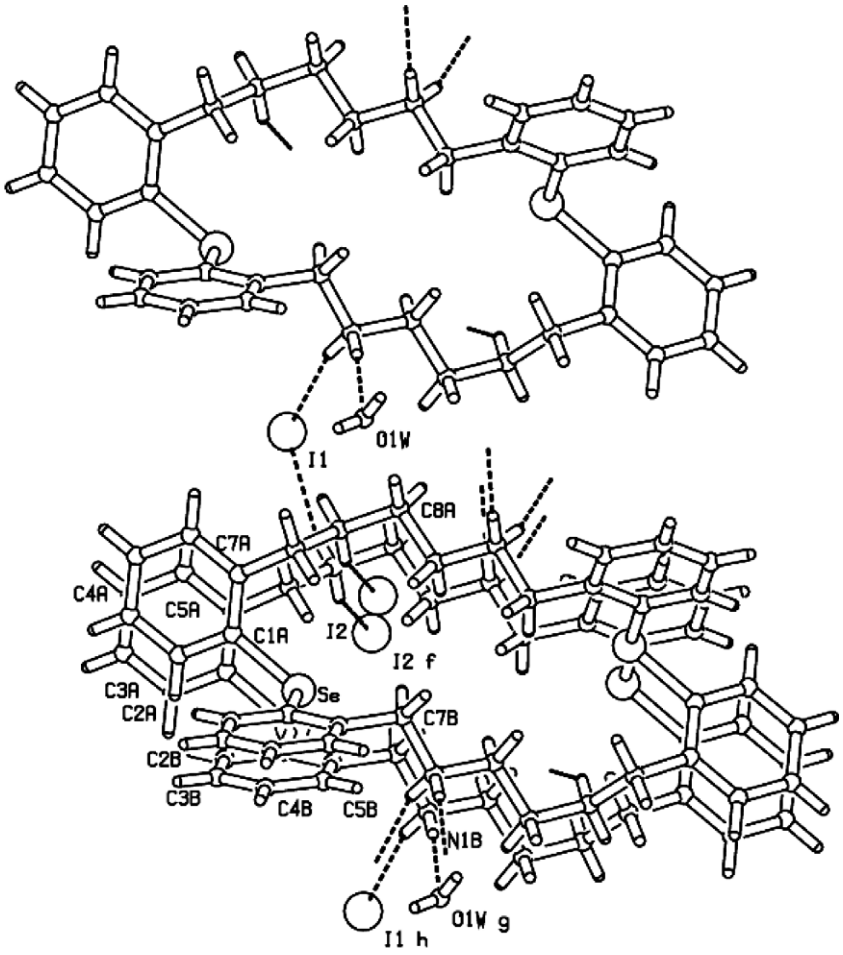

Fig. 4. Packing diagram for compound **6**.

tion away from the TFA ion. The transannular Se...Se distance is 6.8228 Å. Each of the symmetry related N(2) atoms is hydrogen bonded to two oxygen atoms of two different TFA ion. The two oxygen atoms of TFA ion display bifurcated hydrogen bonding with two nitrogen atoms of two different macrocycles at N(2)–O(2) 2.016 Å and N(2)–O(1) 2.798 Å. Both the oxygens of the TFA are involved in the binding which is reminiscent of the metal carboxylate binding in metal adducts [20]. The C–O bond distances [O(1)–C(1T) 1.250(4) Å, O(2)–C(1T) 1.234(4) Å] and O–C–O bond angle [127.5(3)°], compare well with the copper adduct of trifluorocarboxylate [C–O 1.242(11) Å and O–C–O angle 129.6(9)°, respectively] [20]. The same bond lengths are also found in a TFA porphyrin adduct [21]. The two non-protonated nitrogen atoms bend away from the TFA ion. The two symmetry related phenyl rings form π–π stacking interaction along all the axis (*a*,*b*,*c*) at a distance of 3.953 Å within the same molecule. The packing diagram shows a strong π–π stacking interaction between the adjacent molecules at a distance of 3.333 Å. The entire packing system (Fig. 8, Table 6) forms a supramolecular arrangement by hydrogen bonding and strong π stacking interactions between the layers of macrocycle and the anions.

Table 4
Hydrogen bonds for **6** (Å and °)

D–H...A	*d*(D–H)	*d*(H...A)	*d*(D...A)	∠(DHA)
O(1W)–H(1W1)...I(1)#2	0.76	3.21	3.673(8)	122.1
O(1W)–H(1W2)...I(2)#3	0.83	3.08	3.788(13)	144.5
N(1A)–H(1AA)...I(1)	0.90	2.56	3.435(6)	164.3
N(1A)–H(1AB)...I(2)	0.90	2.66	3.472(6)	149.8
N(1B)–H(1BB)...I(1)#4	0.90	2.59	3.466(5)	165.6
N(1B)–H(1BA)...O(1W)	0.90	1.91	2.792(10)	166.5

2.3.5. Molecular structure of compound *16*

The molecular structure of the perchlorate adduct (Fig. 9) shows the macrocycle to be in the hexaprotonated form. The compound contains the ligand **2**, six perchlorate ions and nine water molecules of crystallization. The major axis runs between C(1B)–C(1B) with a distance of 13.589 Å, whereas the minor axis length C(7A) to C(7B) is 5.556 Å. The transannular Se...Se distance is 11.367 Å. Here, the two selenium atoms are bent away from the plane of the macrocycle in the same direction. One of the three symmetry related perchlorate ions is disordered. The disordered ion is extensively bonded to the macrocycle by hydrogen bonding. The nitrogen atoms of the macrocycle have interactions with the disordered perchlorate ions and water mol-

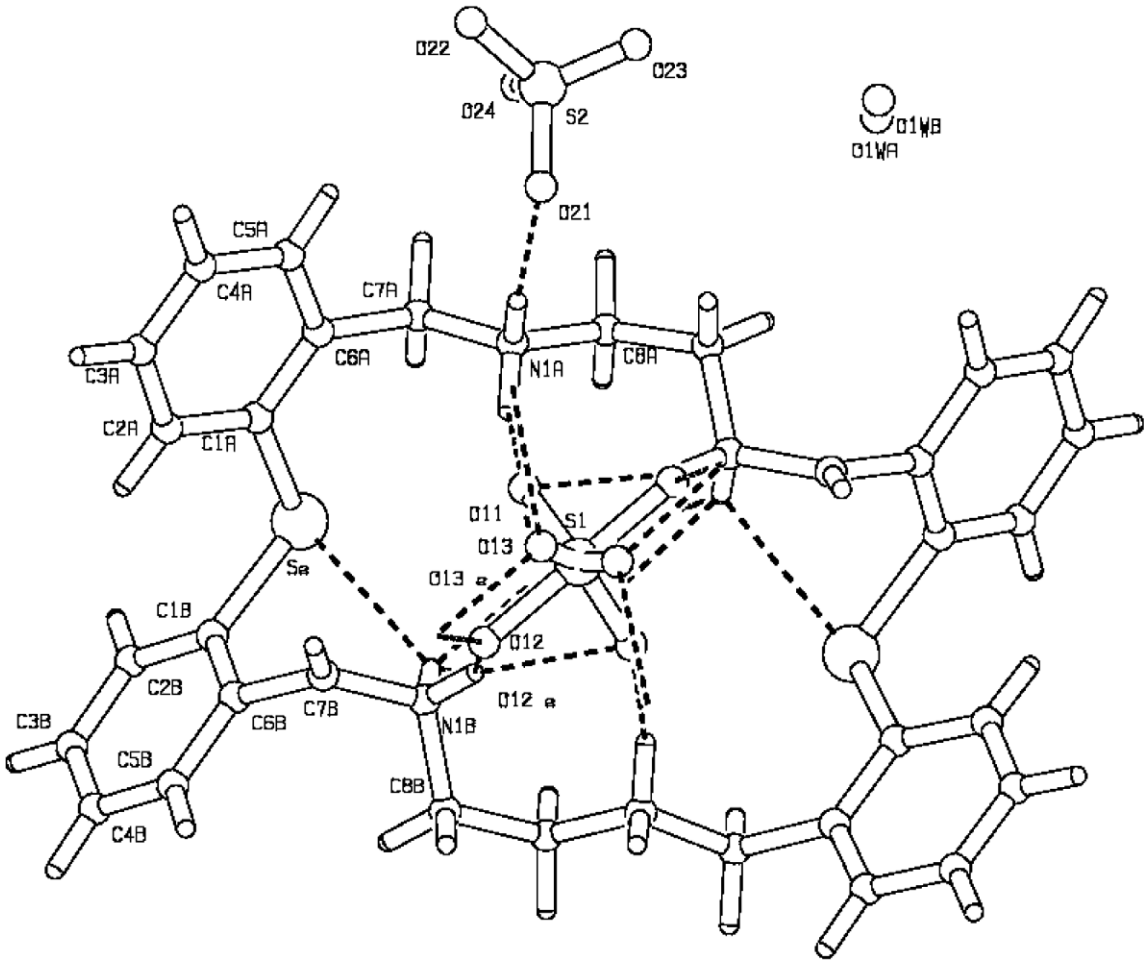

Fig. 5. Overhead view of compound **7**.

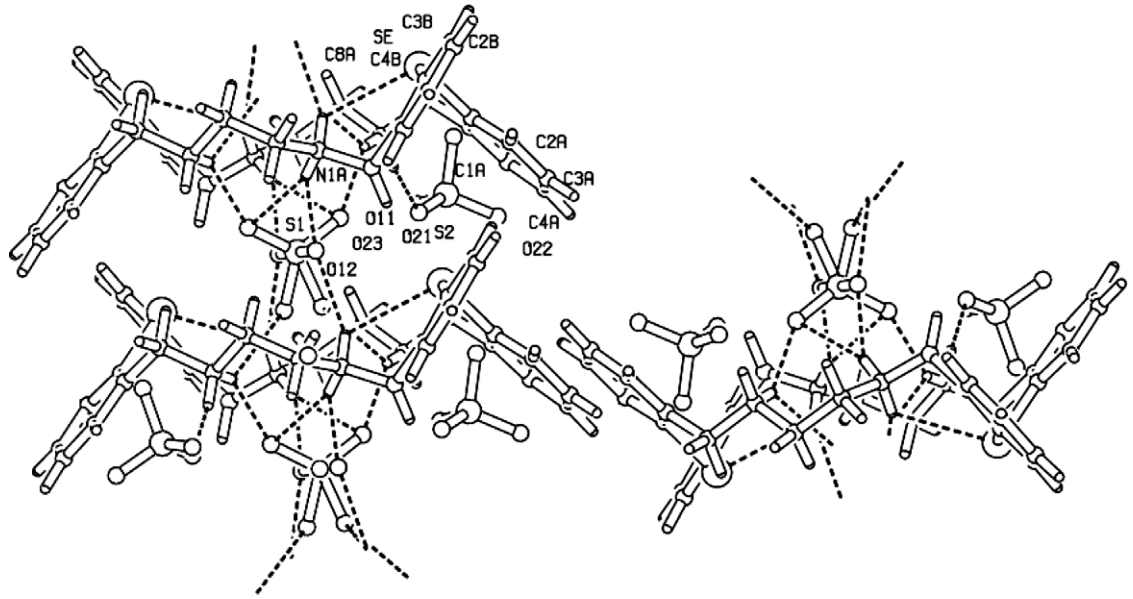

Fig. 6. Packing diagram of compound **7**.

ecules. The hydrogen bond distances (Table 7) between nitrogen atom of the macrocycle and oxygen atoms of perchlorate anion are: (N(1A)...O(13B)#4 2.790(6) Å, N(1A)...O(12A)#4 2.895(6), N(1A)...O(14C)#4 3.327(6), N(1A)...O(2W) 2.711(10), N(1B)...O(11C) 2.640(5), N(1B)...O(11A) 2.961(5), N(1B)...O(14B) 3.228(5),

Table 5
Hydrogen bonds for **7** (Å and °)

D–H...A	*d*(D–H)	*d*(H...A)	*d*(D...A)	∠(DHA)
N(1A)–H(1AA)...O(21)	0.92	1.85	2.739(11)	160.8
N(1A)–H(1AB)...O(11)	0.92	2.04	2.777(10)	136.3
N(1A)–H(1AB)...O(13)#2	0.92	2.60	3.248(14)	128.3
N(1B)–H(1BA)...O(12)	0.92	1.87	2.609(12)	136.3
N(1B)–H(1BA)...O(11)#1	0.92	2.32	3.205(12)	161.6
N(1B)–H(1BA)...O(11)	0.92	2.64	3.372(12)	136.5
N(1B)–H(1BB)...O(13)#2	0.92	1.98	2.714(13)	135.2
N(1B)–H(1BB)...O(12)#2	0.92	2.22	3.047(12)	149.2

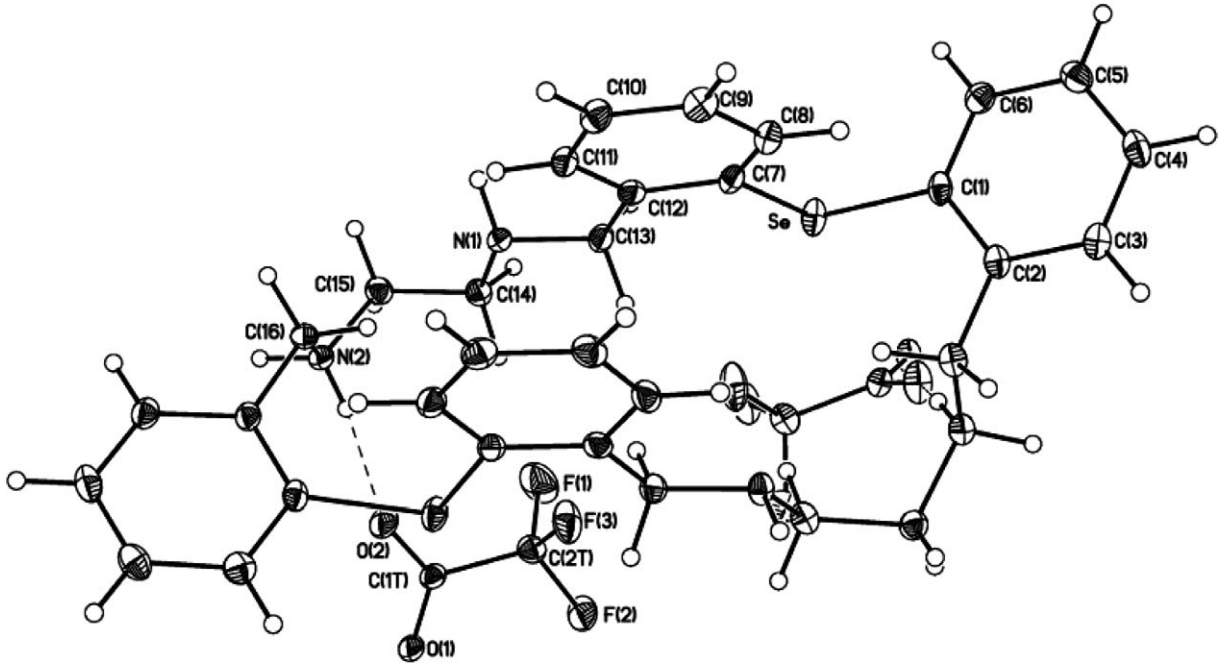

Fig. 7. Side view figure of compound **10**.

N(1B)...O(12B) 3.303(5), N(1B)...O(4W) 2.761(8)). These hydrogen bond distances are well within the reported hydrogen bond distance between nitrogen atom of a protonated cryptand with the encapsulated perchlorate anion [22]. In case of the perchlorate adduct **16**, the hydrogen bond distance between N(1B) and O(11C) {2.640(5)} is smaller, compared to the hydrogen bond distance reported for the perchlorate encapsulated protonated cryptate host [22]. The Cl–O distances (~1.38 Å) are comparable to bound Cl–O anions [22,23]. The other two perchlorate ions do not have direct interaction with the macrocycle frame. Instead, they interact with the nearby water molecules. The entire packing (Fig. 10) system forms a supramolecular arrangement by the hydrogen bonding between the macrocyclic framework.

2.3.6. Molecular structure of compound *18*

In contrast to **10**, the molecular structure (Fig. 11) of the compound shows the macrocycle in the hexaprotonated state. The compound contains the ligand **2**, six trifluroacetate ions and four water molecules. Here, the symmetry related phenyl rings are canted away from the puckered plane of the macrocycle frame of adduct in a *trans* manner. The major axis runs between C(1A)–C(1A) with a distance of 13.349 Å, whereas the minor axis length N(2B) to N(2B) is 4.786 Å. The transannular Se...Se distance is 11.485 Å. Here the two selenium atoms deviate from the plane of nitrogen and carbon atoms at same angle ~98°. The fluorine atoms of the TFA are disordered. These disordered F atoms of the TFA ion show intramolecular as well as intermolecular interactions to oxygen atom of the same molecule and adjacent water molecule, respectively. Out of six trifluroacetate anions, two are extensively bonded to the macrocycle. The TFA ion(A) is bonded to two N–H hydrogen atoms of the macrocycle through hydrogen bonding by one O atom, [N(1B)–O(2A) 2.733(9) Å and N(2B)–O(2A) 2.946(9) Å] and the other oxygen atom is bonded to water molecule [O(1W)–O(1A)#4 2.926(9) Å]. One of the water molecules is bonded to another water molecule and two fluorine

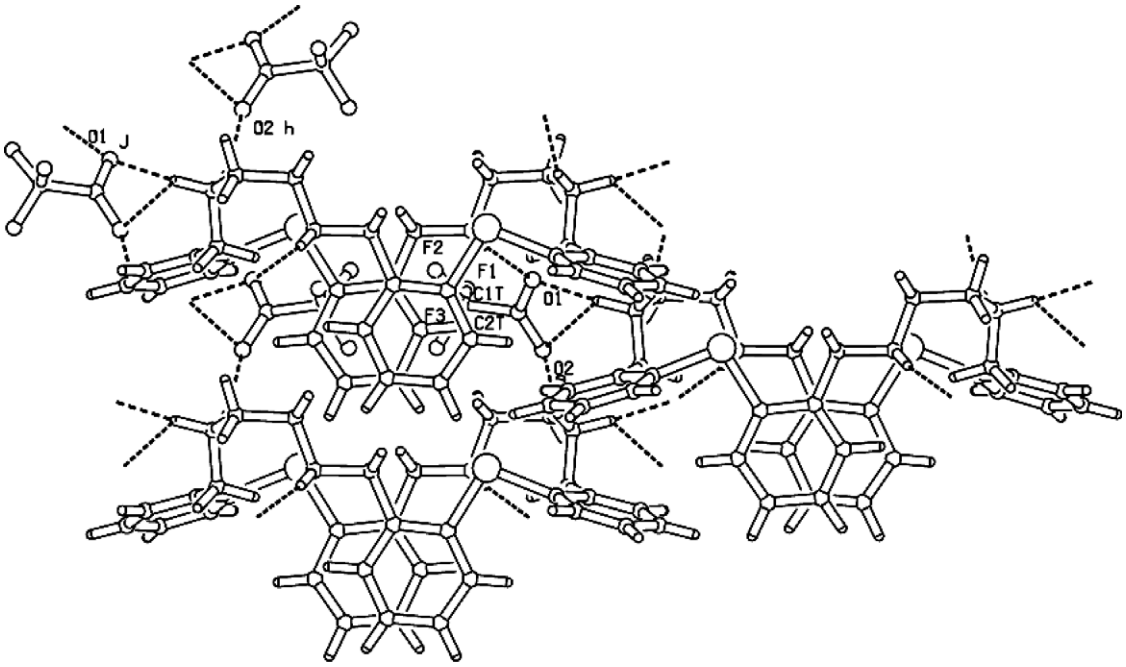

Fig. 8. Packing diagram of compound **10**.

Table 6
Hydrogen bonds for **10** (Å and °)

D–H...A	*d*(D–H)	*d*(H...A)	*d*(D...A)	∠(DHA)
N(1)–H(1N)...O(1)#2	0.91(4)	2.21(4)	3.110(3)	168(3)
N(2)–H(2N1)...O(2)	0.82(3)	2.02(3)	2.777(4)	153(3)
N(2)–H(2N2)...O(1)#3	1.01(4)	1.79(4)	2.798(4)	170(3)
N(2)–H(2N2)...O(2)#3	1.01(4)	2.52(4)	3.116(4)	117(3)

atoms of the TFA(A) and TFA(C). TFA(C) also binds to two N–H hydrogen atoms of two different macrocycles. Although TFA(B) is bonded to two NH atoms of two different macrocycle, it is not bonded to the water molecule. Out of three types of TFA, the TFA(A) anion is extensively bonded to the macrocycle and these hydrogen-bonding interactions have significant effect on the C–O bond length and O–C–O bond angle of TFA ions. The O–C bond lengths in TFA anions (A and B) are in the range of 1.223(10)–1.240(10) Å and the O–C–O bond angles are in the range of 130.0(8)–130.3(9)°, which are close to the metal carboxylate bond length and bond angles [20]. However, TFA(C) has retained the acid bond lengths. Water molecules are extensively hydrogen bonded to anion as well as the macrocycle. The packing diagram (Fig. 12, Table 8) shows the π-stacking interaction (3.858 Å) between the phenyl rings of the adjacent macrocycle. In contrast to **10**, there is absence of the intramolecular π–π stacking interactions in **18**. The packing diagram shows the formation of a supramolecular arrangement of the compound by hydrogen bonding and strong π stacking interaction between layers of macrocycle, the TFA anions and the water molecules.

2.4. Binding study

Information about the binding of the receptors to the anion guests was attempted by the solution studies as well as the solid-state crystallographic data (vide supra). As the ligand is colorless, the determination of the binding constant by competitive UV assay method was attempted. Unfortunately the ligand does not show any binding affinity for the common dyes such as *para*-nitrophenol, which may be due to the small and puckered cavity size of the macrocycles (**1**,**2**).

The binding propensity of the ligand **1** with HBr was attempted by the potentiometric method. The affinities between anion and their polyamine-based receptor were measured in aqueous solution. The protonation constant was determined from titration of the ligand **1,** containing small excess of HBr against the NaOH solution. The pH jump in the titration curve was very sharp, indicating that all the four nitrogen atoms of the macrocycle were deprotonated at a constant pH. The pK_a value has been found out as 5.3 [24].

The determination of the binding constants of polyammonium macrocycle by the NMR titration method was unsuccessful due to the masking of the macrocycle peaks by the peaks of bulky *p*-toluene sulfonic acid anion.

The poor solubility of the protonated macrocycle in protic solvents prompted us to study the binding affinity of the neutral macrocycle towards anions by the NMR titration method. The anions were used as their tetrabutyl ammonium salts. The NMR titration was done in $CDCl_3$. Various amounts of stock solutions of the anionic guest (0.0125 M stock solution) were added to 0.1 cm^3 aliquots of the host (ligand **1**) solution (0.006 M stock solution) and were made

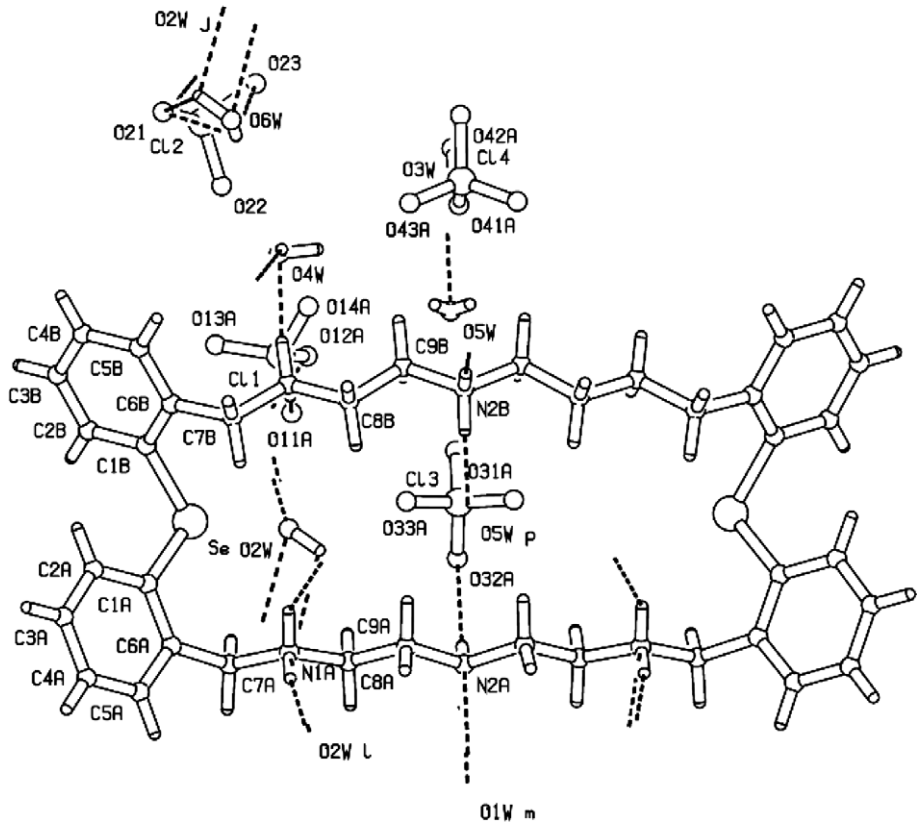

Fig. 9. Overhead view of the molecular structure of compound **16**.

Table 7
Hydrogen bonds for **16** (Å and °)

D–H...A	*d*(D–H)	*d*(H...A)	*d*(D...A)	∠(DHA)
O(1W)–H(1W2)...N(2A)#2	0.849(10)	2.33(5)	2.757(13)	111(4)
O(2W)–H(2W1)...O(6W)	0.851(10)	2.19(8)	2.57(3)	107(6)
O(3W)–H(3W1)...O(41A)#3	0.850(11)	2.13(4)	2.911(11)	153(10)
O(4W)–H(4W2)...O(24)#4	0.850(10)	2.22(3)	2.981(8)	149(5)
O(5W)–H(5W1)...O(12B)#4	0.849(10)	2.36(7)	2.999(5)	133(8)
O(6W)–H(6W1)...O(21)#5	0.850(10)	2.08(5)	2.53(2)	112(4)
O(6W)–H(6W2)...O(2W)	0.850(10)	2.14(11)	2.57(3)	111(10)
N(1A)–H(1AA)...O(13B)#4	0.90	2.00	2.790(6)	146.4
N(1A)–H(1AA)...O(12A)#4	0.90	2.16	2.895(6)	138.8
N(1A)–H(1AA)...O(14C)#4	0.90	2.62	3.327(6)	135.7
N(1A)–H(1AB)...O(2W)	0.90	1.82	2.711(10)	170.2
N(2A)–H(2AD)...O(32A)	0.90	2.31	3.129(9)	152.2
N(2A)–H(2AC)...O(1W)#6	0.90	1.96	2.757(13)	147.4
N(1B)–H(1BA)...O(11C)	0.90	1.76	2.640(5)	165.0
N(1B)–H(1BA)...O(11A)	0.90	2.07	2.961(5)	173.0
N(1B)–H(1BA)...O(14B)	0.90	2.35	3.228(5)	165.6
N(1B)–H(1BA)...O(12B)	0.90	2.66	3.303(5)	129.1
N(1B)–H(1BB)...O(4W)	0.90	1.86	2.761(8)	173.6
N(2B)–H(2BC)...O(5W)	0.90	1.99	2.813(11)	151.8
N(2B)–H(2BD)...O(3W)	0.90	1.83	2.730(13)	176.0

upto 0.6 cm^3 with solvent to maintain a constant volume and thus a constant host concentration.Upon addition of the anions, significant downfield shifts were observed for the NH protons of the receptor. A representative plot for the shift of protons in NMR titration for F^- ion is given in Fig. 13. The binding constants of the neutral macrocycle with F^-, Br^-, I^- and SO_4^{2-} anions have been measured by the NMR titration method. The binding constant was calculated using the EQNMR [25] program. For standardization of the programme EQNMR, the binding constant log K for a known octaaza cryptand for the nitrate ion was determined following the procedure reported by Hynes et al. [22]. The value found out was 3.42 ± 0.43 against the reported value of 3.63.

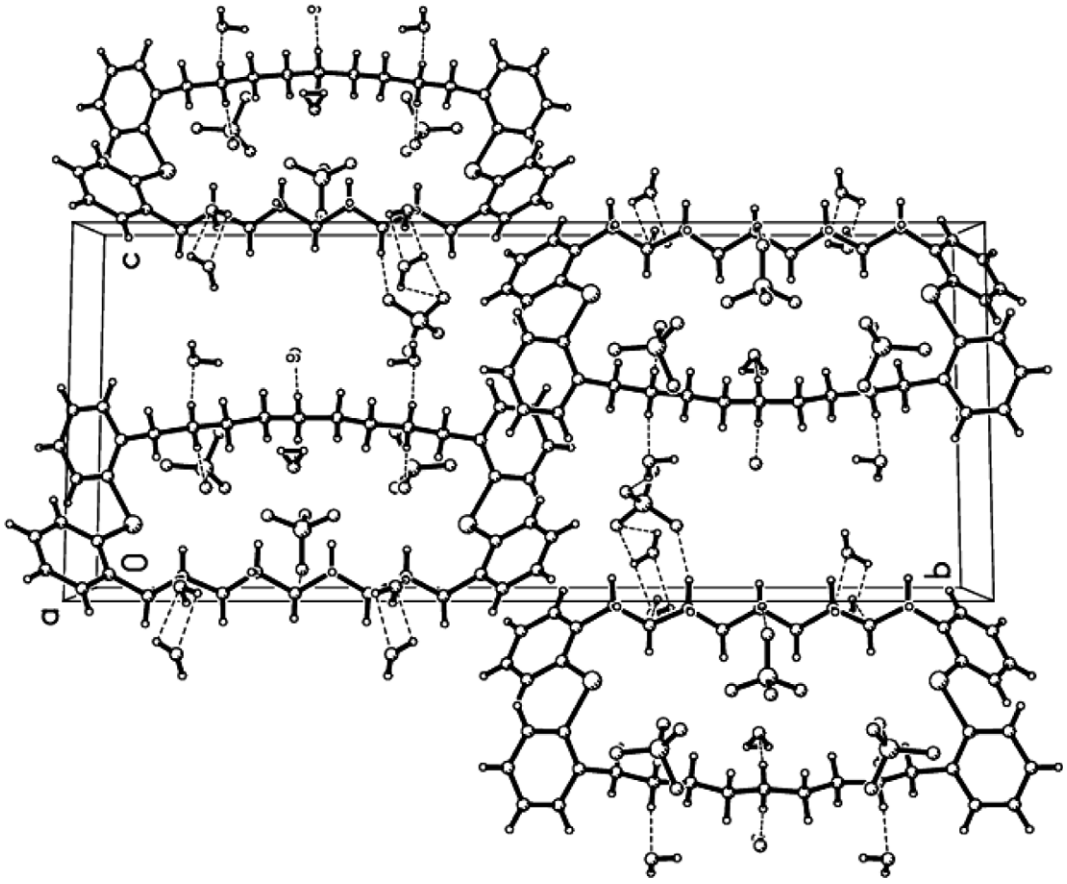

Fig. 10. Packing diagram of compound **16**.

The binding constant $\log K$ values of the neutral macrocycle **1** with halide anions show a small binding affinity towards fluorine ($\log K$ 1.21 ± 0.015) and bromine ($\log K$ 1.95 ± 0.64) compared to the iodide anion ($\log K$ 4.26 ± 0.67). The higher affinity of the neutral macrocycle towards iodide may be due to the affinity of Se towards iodine [14]. The binding constant of the neutral macrocycle towards the sulfate anion (5.12 ± 0.34) is the highest one, which is also higher than the reported sulfate affinity of a hexaprotonated monocycle [4.07(2)] [19]. The hydrogen-bonding interactions in the solution state may contribute to the higher binding affinity of the neutral macrocycle towards sulfate.

3. Conclusion

The ^{77}Se NMR spectra of the anion adducts of the selenaaza macrocycles reveal that in case of the sulfate adduct **7** there is a considerable upfield shift (difference ~241 ppm) of peak position compared to the free ligand, whereas in case of other adducts there is only a marginal shift of the peak positions. This upfield shift in case of **7** can be explained in terms of the short contacts between the sulfate ion and the macrocycle in the solid as well as in the solution state. The ^{77}Se NMR chemical shift and the binding constant indicate that the macrocycle **1** has the highest binding affinity towards the sulfate ion of all the anions studied.

Crystal structures show that the macrocycles **1** and **2** form extensive hydrogen-bonding adducts with the anions, which lie above and below the macrocycle framework. The TFA adduct of **1** afforded the diprotonated form of the macrocycle, whereas all other adducts showed the macrocycles to be fully protonated. Packing diagram of **8** shows extensive hydrogen bonding as well as π stacking interactions between the molecules.

Furthermore, the overall structures of the anion adducts are governed by multiple hydrogen-bonding interactions and short contacts within and outside of the cavity of the macrocycle.

4. Experimental section

4.1. General remarks

Tetrabutylammonium salts of the fluoride, bromide, iodide and sulfate were purchased as reagent grade (Lancaster) and used without further purification. AR grade halic acids were obtained from Merck and used as received. Melting points were recorded in capillary tubes and are

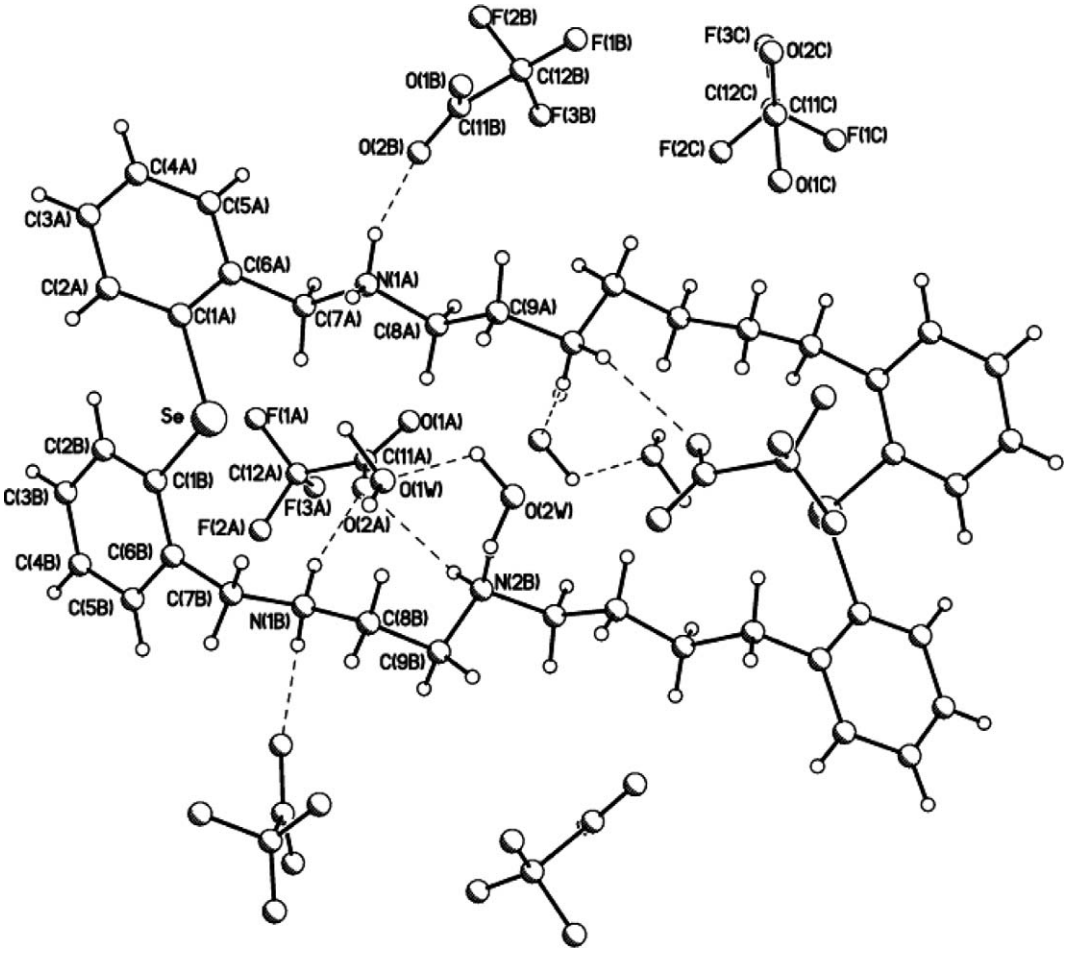

Fig. 11. Overhead view of the molecular structure of compound **18**.

uncorrected. Elemental analysis was performed on Carlo-Erba model 1106 and Eager 300 EA1112 elemental analyzers. IR spectra were recorded as KBr pellets on a Thermo Nicolet Avatar 320 FTIR spectrometer. ^{1}H NMR spectra were obtained at 400 MHz in DMSO, D_2O, or CD_3OD on a Varian spectrometer. ^{77}Se NMR (57.22 MHz) spectra were obtained on Varian 300 and Bruker 500 spectrometer. Chemical shifts are cited with respect to $SiMe_4$ (^{1}H and ^{13}C) and Me_2Se (^{77}Se) as external standard. The Fast Atom Bombardment (FAB) mass spectra were recorded at room temperature with a JEOL SX 102 DA-6000 mass spectrometer data system using xenon (6 kV, 10 mV) as the bombarding gas. ESI-mass spectra were recorded at room temperature on a Q-Tof micro (YA-105) mass spectrometer. The m/z values are quoted with reference to isotopomers containing ^{80}Se; calculated and observed isotope distribution patterns were in good agreement.

4.2. General procedure for the synthesis of protonated binary adducts

The general procedure for the preparation of the binary adducts is as follows. To the methanol solution (20 cm^3) of the ligand **1** (0.2 g, 0.31 mmol) or **2** (0.2 g, 0.27 mmol) the corresponding acids were added dropwise in excess. After 12 h stirring at room temperature the precipitated compound was filtered out. The salts were repeatedly washed with cold water and recrystallized from a ethanol/water mixture.

4.3. Synthesis of compound *3*

Yield: 0.168 g, 70%; m.p. (decomp) >235 °C. $C_{32}H_{40}N_4Se_2F_4 \cdot 2H_2O$ (732.43): due to fluorine content the elemental analysis did not match. ^{1}H NMR (400 MHz, D_2O, 298 K): $\delta = 7.27$–7.58 (m), 4.42 (s), 3.55 (s). ^{77}Se NMR (300 MHz, DMSO-d_6, 298 K): $\delta = 334$ ppm; IR (KBr): $\nu = 3052$, 2923, 2852, 2358, 1466, 766. ESI-MS: $m/z = 737$ (M) 637 [M − (4HF + 2H$_2$O)].

4.4. Synthesis of compound *4*

Yield: 0.21 g, 80%; m.p. (decomp) >258. $C_{32}H_{40}N_4Se_2Cl_4 \cdot 5H_2O$ (870.31): calc. C 44. 16, H 5.79, N 6.34; found: C 44.32, H 5.73, N 6.23. ^{1}H NMR (400 MHz, D_2O, 298 K): 7.32–7.62 (m), 4.55 (s), 3.68 (s). ^{77}Se NMR (500 MHz,

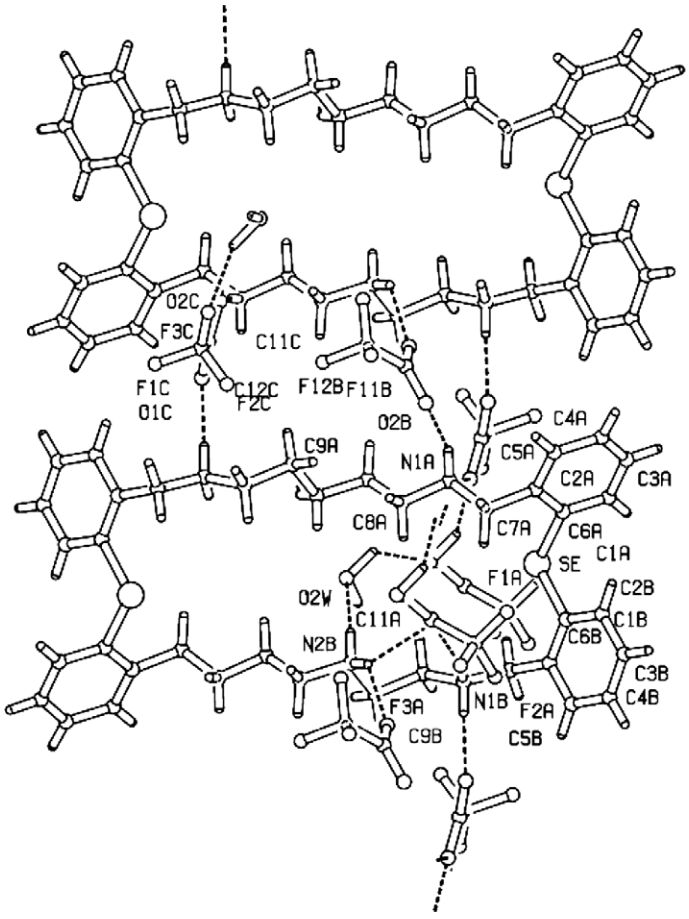

Fig. 12. Packing diagram of compound **18**.

Table 8
Hydrogen bonds for **18** (Å and °)

D–H...A	*d*(D–H)	*d*(H...A)	*d*(D...A)	∠(DHA)
O(2W)–H(2W2)...O(1W)	1.05(5)	2.02(6)	2.735(9)	123(5)
N(1A)–H(1AA)...O(2B)	0.90	1.82	2.648(9)	151.6
N(1A)–H(1AB)...O(2C)#2	0.90	1.89	2.783(9)	172.9
N(1B)–H(1BA)...O(2A)	0.90	1.86	2.733(9)	163.5
N(1B)–H(1BB)...O(1C)#1	0.90	1.92	2.768(8)	156.9
N(2B)–H(2BD)...O(2W)	0.90	1.99	2.847(9)	158.1
N(2B)–H(2BC)...O(1B)#3	0.90	2.08	2.715(10)	126.6
N(2B)–H(2BC)...O(2A)	0.90	2.26	2.946(9)	132.9
O(1W)–H(1W1)...O(1A)#4	1.07(5)	1.87(5)	2.926(9)	167(7)
O(1W)–H(1W1)...F(2A1)#4	1.07(5)	2.30(8)	2.934(18)	116(6)
O(1W)–H(1W1)...F(3A)#4	1.07(5)	2.57(8)	3.213(12)	118(6)
O(1W)–H(1W2)...O(2C)#2	1.06(5)	1.87(6)	2.814(8)	146(6)
O(1W)–H(1W2)...F(3C)#2	1.06(5)	2.53(7)	3.268(15)	126(5)

DMSO-d_6, 298 K): $\delta = 332$. IR (KBr): $v = 3399$, 2924, 2728, 1441, 759. ESI-MS: m/z 795 [M − $4H_2O$], 763 [M − ($4H_2O$ + 3Cl)], 651 [M − ($4H_2O$ + 4Cl)], 635 [M − ($5H_2O$ + 4Cl)].

4.5. Synthesis of compound 5

Yield: 0.14 g, 66%. $C_{32}H_{40}N_4Se_2Br_4 \cdot H_2O$ (976.06): calc. C 39.37, H 4.33, N 5.74; found: C 38.87, H 4.19, N

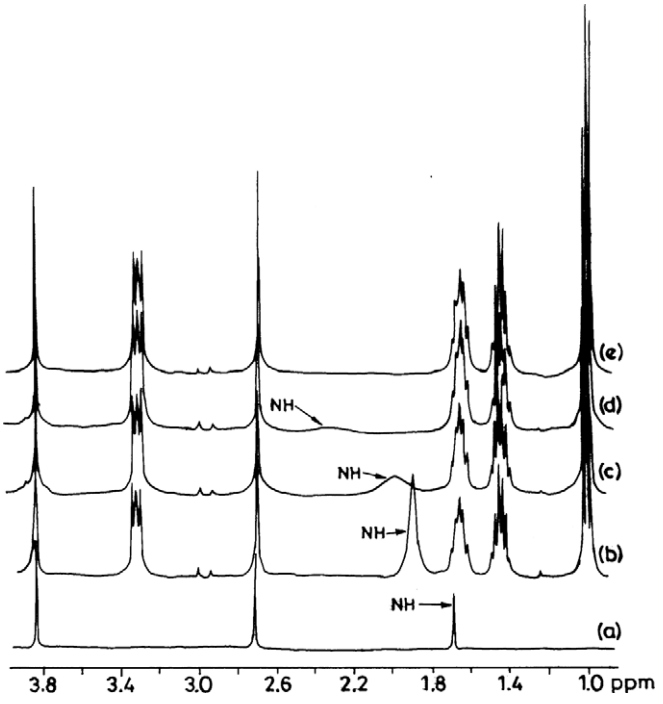

Fig. 13. ^{1}H NMR spectra of the aliphatic region of **1** in $CDCl_3$ showing the shifts of amine protons upon the addition of varying amounts {0 (a), 0.5 (b), 1 (c). 1.5 (d), 3 (e), equiv(s)} of n-Bu_4NF at 25 °C.

5.40. ^{1}H NMR (300 MHz, CD_3OD, 298 K): $\delta = 7.35$–7.74 (m), 4.46 (s), 3.59 (s). ^{77}Se NMR (300 MHz, CD_3OD, 298 K): $\delta = 327$. IR (KBr): $\nu = 1629$, 1561, 1471. FAB-MS: m/z 717 [M − (H_2O + 3Br)], 637 [M − (H_2O + 4Br)].

4.6. Synthesis of compound **6**

Yield: 0.29 g, 93%; m.p. (decomp) >208 °C. $C_{32}H_{40}N_4Se_2I_4 \cdot 2H_2O$ (1182.07): calc. C 32.51, H 3.97, N 4.85; found: C 32.03, H 3.90, N 4.80. ^{1}H NMR (400 MHz, CD_3OD, 298 K): $\delta = 7.19$–7.509 (m), 4.71 (s), 3.97 (s). ^{77}Se NMR (500 MHz, D_2O, 298 K): $\delta = 326$. IR (KBr): $\nu = 3470$, 3411, 2901, 2762, 1432, 763. ESI-MS: m/z = 637 [M − (4I + $2H_2O$)].

4.7. Synthesis of compound 7

Yield: 0.16 g, 54%; m.p. (decomp) >235 °C. $C_{32}H_{40}N_4Se_2O_8S_2 \cdot H_2O$ (848.57): calc. C 45.2, H 4.4, N 6.6, S 7.5; found: C 45.6, H 4.4, N 7.42, S 6.86. ^{1}H NMR (400 MHz, DMSO-d_6, 298 K): $\delta = 7.34$–7.68 (m), 4.36 (s), 3.47 (s). ^{77}Se NMR (500 MHz, DMSO-d_6, 298 K): $\delta = 88$. IR (KBr): $\nu = 3416$, 3054, 2926, 2743, 1459, 1117 (ν_{SO_4}), 756. FAB-MS: m/z 735 [M − H_2SO_4], 635 [M − $2H_2SO_4$].

4.8. Synthesis of compound **8**

Yield: 0.205 g, 60%; m.p. (decomp) >153 °C. $C_{32}H_{40}N_4Se_2O_{16}Cl_4 \cdot H_2O$ (1054.24): calc. C 36.45, H 4.01, N 5.31; found: C, 36.38; H, 4.22; N, 4.96.; ^{1}H NMR (400 MHz, DMSO-d_6, 298 K): $\delta = 7.34$–7.64 (m), 4.75 (s), 3.66 (s). ^{77}Se NMR (300 MHz, D_2O, 298 K): δ 311. IR (KBr): $\nu = 3533$, 2776–3154 (broad multiplet), 1588, 1090, 626. ESI-MS: m/z 891 [M + $2H_2O$–$2ClO_4$], 737 [M + $2H_2O$–$3ClO_4$], 637 [M − ($2H_2O$ + $4ClO_4$)].

4.9. Synthesis of compound **9**

Yield: 0.252 g, 77%; m.p. (decomp) >255 °C. $C_{32}H_{48}N_4Se_2O_{16}P_4$(1026.34): calc. C 37.44, H 4.71, N 5.48; found: C 37.12, H 4.2, N 5.3. ^{1}H NMR (400 MHz, DMSO-d_6, 298 K): $\delta = 7.19$–7.48 (m) 3.95 (s), 2.82 (s). ^{31}P NMR (400 MHz, DMSO-d_6, 298 K): $\delta = -0.506$. ^{77}Se NMR: could not recorded due to poor solubility. IR (KBr): $\nu = 2776$–3015 (broad multiplet), 1621, 2370, 945. ESI-MS: m/z 735 [M − $3H_3PO_4$] 653 [M + H_2O-$4H_3PO_4$].

4.10. Synthesis of compound **10**

Yield: 0.193 g, 80%; m.p. 188–190 °C. $C_{36}H_{38}N_4Se_2O_4F_6$ (862.45): calc. C 50.13, H 4.44, N 6.49; found: C 49.87, H 3.97, N 4.89. ^{1}H NMR (500 MHz, CD_3OD, 298 K): $\delta = 7.18$–7.55 (m), 4.42 (s), 3.63 (s). ^{77}Se NMR (300 MHz, CD_3OD, 298 K): $\delta = 333$. ^{13}C (500 MHz, CD_3OD, 298 K): $\delta = 138$, 135.9, 134, 132, 131, 129.9, 53, 46. IR (KBr): $\nu = 3434$, 3289, 2852, 1650. ESI-MS: m/z 637 [M − $2CF_3COOH$].

4.11. Synthesis of compound **11**

Yield: 0.2 g, 72%; m.p. (decomp) >158 °C. $C_{32}H_{40}N_8Se_2O_{12} \cdot H_2O$ (904.46): calc. C 42.49, H 4.68, N 12.38; found: C 42.27, H 4.44, N 12.38. ^{1}H NMR (300 MHz, DMSO-d_6, 298 K): $\delta = 7.34$–7.64 (m), 4.53 (s), 3.60 (s) ^{77}Se NMR (300 MHz, D_2O, 298 K): $\delta = 310$. IR (KBr): $\nu = 2776$–3015 (broad multiplet), 1588, 1383. ESI-MS: 783 [M − $2HNO_3$], 697 [M − $3HNO_3$ − H_2O].

4.12. Synthesis of compound **12**

Yield: 0.22 g, 78%; m.p. (decomp) >218 °C. ^{1}H NMR (400 MHz, DMSO-d_6, 298 K): $\delta = 7.32$–7.58 (m), 4.47 (s), 3.52 (s). ^{77}Se NMR (300 MHz, D_2O, 298 K): $\delta = 310$ ppm. IR (KBr): $\nu = 3431$, 3007, 2784, 2442, 1876, 1521, 1468, 1052, 749, 659.

4.13. Synthesis of compound **13**

Yield: 0.216 g, 80%; m.p. (decomp) >276 °C. $C_{36}H_{52}N_6Se_2Cl_6 \cdot 2H_2O$ (975.33): calc. C 44.33, H 5.78, N 8.61; found: C 43.89, H 5.86, N 8.38. ^{1}H NMR (400 MHz, DMSO-d_6, 298 K): $\delta = 7.23$–7.53 (m), 4.45 (s), 3.57 (m). ^{77}Se NMR (300 MHz, CD_3OD, 298 K): $\delta = 312$. IR (KBr): $\nu = 3404$, 2924, 2852, 2721, 1440, 763. ESI-MS: m/z 749 [M − (6Cl + H_2O)], 723 [M − (6Cl + $2H_2O$)].

4.14. Synthesis of compound **14**

Yield: 0.398 gm, 80%; m.p. (decomp) >220 °C. $C_{36}H_{52}N_6Se_2I_6$ (1488.01): calc. C 29.05, H 3.52, N 5.64; found: C 29.56, H 3.65, N 6.21. ^{1}H NMR (400 MHz, D_2O, 298 K): $\delta = 7.34$–7.63 (m), 4.61 (s), 3.70 (m). ^{77}Se NMR (500 MHz, CD_3OD, 298 K): $\delta = 330$. IR (KBr): $\nu = 3426$, 2928, 2766, 1439, 754. ESI-MS: m/z 979 [M − 4I], 875 [M + H_2O − 5I], 852 [M − 5I], 721 [M − 6I].

4.15. Synthesis of compound **15**

Yield: 0.218 g, 60%; m.p. (decomp) >215 °C. $C_{36}H_{58}N_6Se_2O_{24}S_6 \cdot H_2O$ (1325): calc.: C 32.63, H 4.41, N 6.34, S 14.51; found: C 33.03, H 3.91, N 7.4, S 12.42. ^{1}H NMR (400 MHz, D_2O, 298 K): $\delta = 7.19$–7.63 (m), 4.51 (s), 3.66 (m). ^{77}Se NMR (300 MHz, DMSO-d_6, 298 K): $\delta = 323$. IR (KBr): $\nu = 3428$, 3016, 2803, 1442, 1186, 1051.

4.16. Synthesis of compound **16**

Yield: 0.212 g, 50%. $C_{36}H_{50}N_6Se_2O_{24}Cl_6 \cdot 9H_2O$ (1412.5): calc. C 30.61, H 4.85, N 5.94; found: C 29.14, H 4.23, N 5.39. ^{1}H NMR (400 MHz, CD_3OD, 298 K): δ 7.34–7.59 (m), 4.53 (s), 3.60 (m); ^{77}Se NMR (500 MHz, D_2O, 298 K): $\delta = 314$. IR (KBr): $\nu = 3512$, 2959, 1443, 1088, 756, 626. ESI-MS: m/z 1023 [M − ($3HClO_4$ + $9H_2O$)], 923 [M − ($4HClO_4$ + $9H_2O$)], 823 [M − (5HClO4 + $9H_2O$)].

4.17. Synthesis of compound **17**

Yield: 0.311 g, 70%; m.p. (decomp) >244 °C. $C_{36}H_{66}N_6Se_2O_{24}P_6 \cdot 8H_2O$ (1454.64): calc. C 29.72, H 5.68, N 5.77; found: C 29.40, H 4.48, N 5.25. IR (KBr): $\nu = 3417$, 2924, 2388, 1469, 975, 751. ^{1}H NMR (400 MHz, D_2O, 298 K): $\delta = 7.32$–7.58 (m), 4.50 (s), 3.55 (m). ^{77}Se NMR: (could not be recorded due to solubility problem). ^{31}P NMR (400 MHz, DMSO-d_6, 298 K): $\delta = -1.045$. ESI-MS: m/z 1035.05 [M − ($7H_2O + 3PO_4$)], 919.1 [M − (4 $H_3PO_4 + 8H_2O$)], 837 [M − ($7H_2O + 5PO_4$)], 821 [M − ($7H_2O + 6PO_4$)], 723 [M − ($8H_2O + 6PO_4$)].

4.18. Synthesis of compound **18**

Yield: 0.238 g, 60%; m.p. (decomp) >278 °C. $C_{48}H_{54}N_6Se_2O_{12}F_{18} \cdot 3H_2O$ (1460.74): calc. C 39.46, H 4.14, N 5.75; found: C 39.26, H 3.91, N 5.68. IR (KBr): $\nu = 3448$, 3024, 2924, 2851, 1675,1471, 1203, 1127, 799. ^{1}H NMR (300 MHz, CD_3OD, 298 K): $\delta = 7.32$–7.63 (m), 4.46 (s), 3.38 (m). ^{13}C NMR (500 MHz, CD_3OD, 298 K): $\delta = 163$, 136, 133.9, 133.5, 132.7, 132.6, 130.8, 119, 116, 52, 45. ^{77}Se (500 MHz, CD_3OD, 298 K): $\delta = 315$.

4.19. Synthesis of compound **19**

Yield: 0.32 g, 70%; m.p. (decomp) >272 °C. $C_{36}H_{52}N_6Se_2N_6O_{18} \cdot H_2O$ (1116.62): calc. C 38.723, H 4.87, N 15.05; found: C 38.85, H 4.56, N 16.51. IR (KBr): $\nu = 3426$, 3022, 2799, 1601, 1383, 1303, 1027, 819, 758, 721; ^{1}HNMR (400 MHz, D_2O, 298 K): $\delta = 7.33$–7.59 (m), 4.52 (s), 3.60 (m). ^{77}Se NMR: (could not be recorded due to solubility problem) ESI-MS: m/z 909 [M − $3HNO_3$], 866 [M − $4NO_3$], 839 [M − ($4NO_3 + H_2O$)], 808 [M − $5NO_3$], 779 [M − ($5NO_3 + H_2O$)], 721 [M − ($6NO_3 + H_2O$)].

4.20. X-ray crystallographic study

The diffraction measurements for the ligands as well as adducts were performed at room temperature on a 'Bruker P4' diffractometer with graphite-monochromated Mo Kα radiation ($\lambda = 0.71073$ Å). The data were corrected for Lorentz, polarization and absorption effects The structures were determined by routine heavy-atom using SHELXS 97 [26] and Fourier methods and refined by full-matrix least squares with the non-hydrogen atoms anisotropic and hydrogen with fixed isotropic thermal parameters of 0.07 Å^2 by means of the SHELXL 97 [27] program. The hydrogens were partially located from difference electron-density maps and the rest were fixed at predetermined positions. Scattering factors were from common sources [28].

5. Supplementary data

CCDC Nos. 254395 (**5**), 254450 (**6**), 254451 (**7**), 254452 (**10**), 254453 (**16**), and 253454 (**18**) contain the supplementary crystallographic data for this paper. These data can be obtained free of charge at www.ccdc.cam.ac.uk/conts/retrieving.html [or from the Cambridge Crystallographic Data Centre, 12, Union Road, Cambridge CB2 1EZ, UK; fax: (internat.) +44 1223/336 033; e-mail: deposit@ccdc.cam.ac.uk].

Acknowledgements

We are grateful to the Department of Science and Technology (DST), New Delhi for funding this work. We are grateful to Prof. M.J. Hynes for providing us the EQNMR programme and helpful suggestions. Additional help from the SAIF, Indian Institute of Technology (IIT), Bombay for 300 MHz NMR spectroscopy, RSIC, CDRI Lucknow for mass recording facility, department of chemistry, IIT Bombay for ESI-MS facility and 400 MHz NMR spectroscopy and Tata Institute of Fundamental Research (TIFR), Bombay for 500 MHz NMR spectroscopy is gratefully acknowledged.

References

[1] (a) F.P. Schimddchen, M. Berger, Chem. Rev. 97 (1997) 1609;
(b) P.D. Beer, D.K. Smith, Anion binding and recognition by inorganic based receptors, Prog. Inorg. Chem. 46 (1999) 1;
(c) P.A. Gale, Coord. Chem. Rev. 213 (2001) 79;
(d) P.D. Beer, P.A. Gale, Angew. Chem. Int. Ed. 40 (2001) 486;
(e) D.M. Roundhill, H.F. Koch, Chem. Soc. Rev. 31 (2002) 60;
(f) R.J. Fitzmaurice, G.M. Kyne, D. Douheret, J.D. Kilburn, J. Chem. Soc. Perkin Trans. 1 (2002) 841;
(g) P.A. Gale, Coord. Chem. Rev. 240 (2003) 191;
(h) K. Choi, A.D. Hamilton, Coord. Chem. Rev. 240 (2003) 101.
[2] P.D. Beer, E.J. Hayes, Coord. Chem. Rev. 240 (2003) 167, and references therein.
[3] J.L. Sessler, S. Camiolo, P.A. Gale, Coord. Chem. Rev. 240 (2003) 17, and references therein.
[4] M.D. Best, S.L. Tobey, E.V. Anslyn, Coord. Chem. Rev. 240 (2003) 3, and references therein.
[5] (a) C.R. Bondy, S.J. Loeb, Coord. Chem. Rev. 240 (2003) 77, and references therein;
(b) J.L. Sessler, E. Katayev, G.D. Pantos, Y.A. Ustynyuk, Chem. Commun. (2004) 1276.
[6] J.M. Llinares, D. Powell, K. Bowman-James, Coord. Chem. Rev. 240 (2003) 57, and references therein.
[7] (a) G. Mugesh, A. Panda, H.B. Singh, R.J. Butcher, Chem. Eur. J. 5 (1999) 1411;
(b) S. Kumar, K. Kandasamy, H.B. Singh, G. Wolmershäuser, R.J. Butcher, Organometallics 23 (2004) 4199;
(c) S.S. Zade, S. Panda, H.B. Singh, R.B. Sunoj, R.J. Butcher, J. Org. Chem. 70 (2005) 3693.
[8] (a) D.B. Werz, B.J. Rausch, R. Gleiter, Tetrahedron. Lett. 43 (2002) 5767;
(b) H. Komatsu, M. Iwaoka, S. Tomoda, J. Chem. Soc., Chem. Commun. (1999) 205;
(c) M. Iwaoka, H. Komatsu, T. Katsuda, S. Tomoda, J. Am. Chem. Soc. 126 (2004) 5309;
(d) N. Sudha, H.B. Singh, Coord. Chem. Rev. 135/136 (1994) 469.
[9] W. Nakanishi, S. Hayashi, Phosphorus Sulfur Silicon Relat. Elem. 177 (2002) 1833.
[10] T. Harada, H. Yoshida, K. Ohno, H. Matsuura, J. Zhang, M. Iwaoka, S. Tomoda, J. Phys. Chem. A 105 (2001) 4517.
[11] M. Iwaoka, H. Komatsu, T. Katsuda, S. Tomoda, J. Am. Chem. Soc. 124 (2002) 1902.

[12] W.-W. du Mont, A. Martens-von Salzen, F. Ruthe, E. Seppala, G. Mugesh, F.A. Devillanova, V. Lippolis, N. Kuhn, J. Organomet. Chem. 623 (2001) 14.
[13] Y. Liu, C.-C. You, Y. Chen, T. Wada, Y. Inoue, J. Org. Chem. 64 (1999) 7781.
[14] H. Citeau, K. Kirschbaum, O. Conard, D.M. Giolando, Chem. Commun. (2001) 2006.
[15] (a) A. Panda, S.C. Menon, H.B. Singh, R.J. Butcher, J. Organomet. Chem. 623 (2001) 87;
(b) A. Panda, S.C. Menon, H.B. Singh, C.P. Morley, R. Bachman, T.M. Cocker, R.J. Butcher, Eur. J. Inorg. Chem. (2005) 1114.
[16] (a) S.C. Menon, H.B. Singh, R.P. Patel, S.K. Kulshreshtha, J. Chem. Soc., Dalton. Trans. (1996) 1203;
(b) S.C. Menon, A. Panda, H.B. Singh, R.J. Butcher, Chem. Commun. (2000) 143;
(c) S.C. Menon, A. Panda, H.B. Singh, R.P. Patel, S.K. Kulshreshtha, W.L. Darby, R.J. Butcher, J. Organomet. Chem. 689 (2004) 1452;
(d) S. Panda, H.B. Singh, R.J. Butcher, Chem. Commun. (2004) 322.
[17] H.Z. Sommer, H.I. Lipp, L.L. Jackson, J. Org. Chem. 36 (1971) 824, and references therein.
[18] (a) D.A. Nation, J. Reibenspies, A.E. Martell, Inorg. Chem. 35 (1996) 4597;
(b) A. Llobet, J. Reibenspies, A.E. Martell, Inorg. Chem. 33 (1994) 5946.
[19] T. Clifford, A. Danby, J.M. Linares, S. Mason, N.W. Alcock, D. Powell, J.A. Aguilar, E. García-España, K. Bowman-James, Inorg. Chem. 41 (2001) 47100.
[20] R.J. Doedens, Progress in Inorganic Chemistry, vol. 21, John Wiley and Sons, New York, 1976, p. 209.
[21] S.J. Narayanan, B. Sridevi, T.K. Chandrasekhar, A. Vij, R. Roy, J. Am. Chem. Soc. 121 (1999) 9053.
[22] M.J. Hynes, B. Maubert, V. McKee, R.M. Town, J. Nelson, J. Chem. Soc., Dalton Trans. (2000) 2853.
[23] B.M. Maubert, J. Nelson, V. McKee, R.M. Town, I. Pál, J. Chem. Soc., Dalton Trans. (2001) 1395.
[24] P. Atkins, J. de Paula, Physical Chemistry, Oxford University Press, 2002 (Chapter 9).
[25] M.J. Hynes, J. Chem. Soc., Dalton Trans. (1993) 311.
[26] G.M. Sheldrick, SHELXS-97, Program for Crystal Structures Solution, University of Göttingen, 1990.
[27] G.M. Sheldrick, SHELXL-97; Program for Crystal Structure Refinement, University of Göttingen, Germany, 1997.
[28] International Tables for X-ray Crystallography, vol. 1, Kynoch Press, Birmingham, 1974, p. 99 and 149.